Control of a class of multibody underactuated mechanical systems with discontinuous friction using sliding-mode

Yang Liu[a,*]

[a] College of Engineering Mathematics and Physical Sciences, University of Exeter, Harrison Building, North Park Road, Exeter, EX4 4QF, UK

Abstract

This paper studies sliding-mode control of a class of multibody underactuated systems with discontinuous friction presenting on the unactuated configuration variable with consideration of parametric uncertainties. Global motion for this class system including sticking, stick-slip, and slip regimes are analyzed, and their corresponding equilibria are identified. Our control objective is to avoid the sticking and stick-slip regimes while track a desired velocity in the slip regime. The proposed sliding-mode controllers are robust to parametric uncertainties, and their stabilities are proved by using the Lyapunov direct method. Two examples, a mass-spring-damping system and a drill-string system, are used to demonstrate the validity of the proposed controllers.

Keywords: underactuated system, sliding-mode control, friction, stick-slip, parametric uncertainty.

1. Introduction

Underactuation is a special attribute of the system with fewer independent control inputs than the degrees of freedom (DOF) to be controlled. It causes the control issues which cannot be solved by traditional control theory. The literature for control of underactuation is vast, and most of the systems with such an attribute are mechanical. In the early 90's, the research on control of underactuation originally started from the interest on nonholonomic manipulator (Oriolo and Nakamura, 1991). Later on, extensive underactuated systems were studied, such as mobile robot (Yue et al., 2010), underwater vehicle (Egeland et al., 1996), surface vessel (Ghommam et al., 2010), biped walking robot (Hu et al., 2010), and so on. In the late 90's, the classification and control of a class of underactuated systems were of great interest to many researchers (Spong, 1996; Reyhanoglu et al., 1999). For example, the classification was systematically studied by Olfati-Saber (2001), and a detailed review of underactuated systems and their control methods were done by Liu and Yu (2013). However, most of the studies up to date were on the 2-DOF systems or with a limited number of DOF (Li et al., 2009; She et al., 2012), and less attention has been paid to multi-DOF systems (Ashrafiuon and Erwin, 2008), although they are important in many practical applications (Gosselin et al., 2008; Liu, 2014). On the other hand, friction was not considered as a major factor in most of the previous studies, despite it is ubiquitous in mechanical systems. In some applications, friction is the main source causing undesired oscillations (Olsson and Åström, 2001; Liu, 2014), and understanding system dynamics under such an effect becomes essential. Therefore, this paper is devoted to study a class of multibody underactuated systems with discontinuous friction, and propose control strategies for such a special class system using sliding-mode.

*Corresponding author. Tel. +44-7879665278, e-mail: yliu720@gmail.com.

Recently, sliding-mode control of underactuated systems has attracted considerable attention, e.g. satellite (Ashrafiuon and Erwin, 2005), surface vessel (Fahimi, 2007; Ashrafiuon et al., 2008), biped robot (Nikkhah et al., 2007), overhead crane (Almutairi and Zribi, 2009), ball and beam system (Almutairi and Zribi, 2010), wheeled inverted pendulum (Huang et al., 2010; Xu and Özgüner, 2008), networked control system (Liu et al., 2016), and so on. Particularly, sliding-mode control of a class of underactuated systems is of greater interest to many researchers. For example, Wang et al. (2004) studied a hierarchical sliding-mode control method with two levels of sliding surface for a class of second-order underactuated systems with consideration of external disturbances. Hao et al. (2008) developed an incremental sliding-mode control strategy with multi-level of sliding surface for a class of underactuated systems with mismatched uncertainties. Parametric uncertainties and external disturbances have been considered by Xu and Özgüner (2008) using sliding-mode control. The proposed controller could globally stabilize the systems which do not satisfy the Brockett's necessary conditions (Brockett, 1983) but must be strict in a cascade form. Sankaranarayanan and Mahindrakar (2009) studied a sliding-mode controller for a class of underactuated systems with parametric uncertainties by proposing a switching surface design. It should be noted that the friction in these studies was simplified as a damping resistant force which was proportional to velocity. Discontinuous friction model was only used by Martinez and Alvarez (2008) and Martinez et al. (2008) for a class of second-order underactuated systems. Therefore, we could conclude that most of the sliding-mode controllers were developed for second-order underactuated systems considering simplified friction model. Furthermore, discontinuous friction model may lead to unavailability of global stabilization, so a careful control design for a valid desired equilibrium is crucial. In this paper, we will consider the condition when global stabilization is unavailable for a class of multibody underactuated systems due to discontinuous friction.

This paper studies sliding-mode control of a class of multibody underactuated systems with parametric uncertainties and considering discontinuous friction on unactuated variable. The first contribution of this paper is to analyze the global motion regimes and their corresponding equilibria for this type system. We have found that the motion of these systems could be divided into three regimes while most of the current studies only has one (e.g. Ashrafiuon and Erwin, 2008). The second contribution of this paper is that two new smooth functions for reducing chattering effect have been proposed. Although Liu (2014) has studied the proposed sliding-mode controllers using an underactuated drill-string system, this paper is devoted to generalize these controllers to a class of this type systems. Particularly, discontinues friction models and system stability, which have not been included in Liu (2014), will be studied in this paper. Furthermore, a typical mass-spring-damping system, which is a generalized mathematical model representing a number of mechanical systems, e.g. servo system (Olsson and Åström, 2001), will also be considered in this paper.

The rest of this paper is organized as follows. In Section 2, dynamics of a class of underactuated mechanical systems is introduced, and the friction model adopted in this paper is studied. In Section 3, three motion regimes are identified and their corresponding equilibria are analyzed. In Section 4, three sliding-mode controllers are studied and their stabilities are proved by using the Lyapunov direct method. Simulation results are given in Section 5 using a mass-spring-damping system and a drill-string system in order to validate the effectiveness and robustness of the proposed controllers. Finally, some conclusions are drawn in Section 6.

2. Dynamics of a class of underactuated mechanical systems

Consider a single-input and multi-output mechanical system represented by

$$D\ddot{q} + C\dot{q} + Kq + F = U, \tag{1}$$

where $q = [q_1,\ q_2,\ q_3,\ ...,\ q_{n-1},\ q_n]^T \in \Re^{n\times 1}$ is state vector, $D = \text{diag}(d_1,\ d_2,\ d_3,\ ...,\ d_{n-1},\ d_n)$ $\in \Re^{n\times n}$ is inertia matrix, $C \in \Re^{n\times n}$ is the damping matrix given by

$$C = \begin{bmatrix} c_1 & -c_1 & 0 & \cdots & 0 & 0 & 0 \\ -c_1 & c_1+c_2 & -c_2 & \cdots & 0 & 0 & 0 \\ \vdots & \vdots & \vdots & \ddots & \vdots & \vdots & \vdots \\ 0 & 0 & 0 & \cdots & -c_{n-2} & c_{n-2}+c_{n-1} & -c_{n-1} \\ 0 & 0 & 0 & \cdots & 0 & -c_{n-1} & c_{n-1} \end{bmatrix},$$

$K \in \Re^{n\times n}$ is the stiffness matrix given by

$$K = \begin{bmatrix} k_1 & -k_1 & 0 & \cdots & 0 & 0 & 0 \\ -k_1 & k_1+k_2 & -k_2 & \cdots & 0 & 0 & 0 \\ \vdots & \vdots & \vdots & \ddots & \vdots & \vdots & \vdots \\ 0 & 0 & 0 & \cdots & -k_{n-2} & k_{n-2}+k_{n-1} & -k_{n-1} \\ 0 & 0 & 0 & \cdots & 0 & -k_{n-1} & k_{n-1} \end{bmatrix},$$

where d_i, c_i, and k_i $(i = 1, 2, 3, \cdots)$ are constant, $F = [0,\ 0,\ \cdots,\ f]^T \in \Re^{n\times 1}$ is friction vector, $U = [u,\ 0,\ \cdots,\ 0]^T \in \Re^{n\times 1}$ is the vector for external control input, and f is the discontinuous friction on n^{th} configuration variable, q_n given by

$$f = \begin{cases} f_r & \text{if } |\dot{q}_n| < \zeta \text{ and } |f_r| \le f_s, \\ f_s \text{sgn}(f_r) & \text{if } |\dot{q}_n| < \zeta \text{ and } |f_r| > f_s, \\ \mu_d \Lambda\, \text{sgn}(\dot{q}_n) & \text{if } |\dot{q}_n| \ge \zeta, \end{cases} \tag{2}$$

where f_r is a reaction force given by

$$f_r = c_{n-1}(\dot{q}_{n-1} - \dot{q}_n) + k_{n-1}(q_{n-1} - q_n),$$

ζ is a small positive constant, $f_s = \mu_s \Lambda$ is static friction, μ_s is static friction coefficient, Λ is the force depending on the weight of n^{th} body of the system, and μ_d is the sliding friction coefficient given by

$$\mu_d = \mu_c + (\mu_s - \mu_c)e^{-\gamma|\dot{q}_n|/v_f},$$

where μ_c is Coulomb friction coefficient, $0 < \gamma < 1$ is the constant defining velocity decreasing rate for f, and v_f is a velocity constant.

Based on the discontinuous friction model, the following three phases for the motion of n^{th} body are considered.

- Sticking phase ($|\dot{q}_n| < \zeta$ and $|f_r| \le f_s$): the velocity $\dot{q}_n$ is less than the small positive constant ζ, and the reaction force f_r is less or equals to the static friction f_s. In the sticking phase, the n^{th} body is considered as stationary.

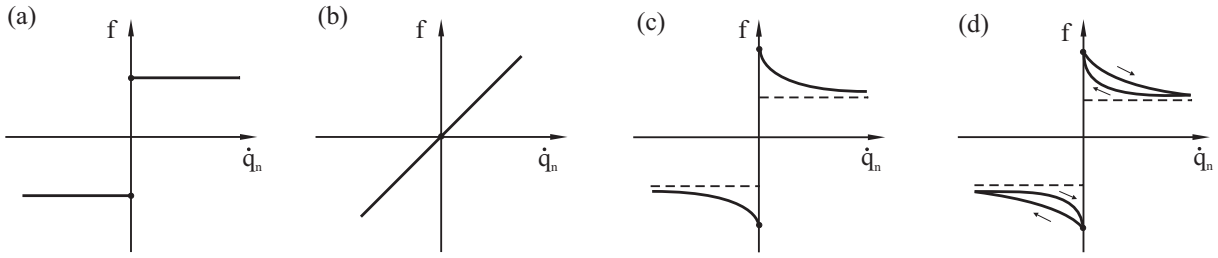

Figure 1: Friction models: (a) Coulomb friction; (b) viscous damping friction; (c) Stribeck friction; (d) seven-parameter friction.

- Stick-to-slip transition phase ($|\dot{q}_n| < \zeta$ and $|f_r| > f_s$): the velocity $\dot{q}_n$ is still less than the constant ζ, but the reaction force f_r is greater than the static friction f_s. So the n^{th} body just begins to move from stationary.

- Slip phase ($|\dot{q}_n| \geq \zeta$): the velocity $\dot{q}_n$ is equal or greater than the constant ζ, and the calculation of friction force includes the sliding friction coefficient μ_d and the weight-related force Λ.

It is known that various friction models shown in Fig. 1 were used for different application scenarios. The Coulomb friction (Fig. 1(a)) is the simplest friction model providing the first approximation of universal friction contact which has been applied to the transmission of a ball and beam system (Márton, 2008), the microrobotic platform (Vartholomeos and Papadopoulos, 2005), and the vibro-impact moling system (Ho et al., 2011). In these applications, friction does not play a major role in system dynamics. In the presence of thin lubricant, viscous damping friction (Fig. 1(b)) which takes into account the viscosity of lubricated contact was frequently employed, e.g. the cart-pole system (Muskinja and Tovornik, 2006), the snake robot (Liljebäck et al., 2011), and the bipedal robot (Hamed and Grizzle, 2014). When the lubricant becomes thicker and the contacting bodies are completely separated, the Stribeck friction (Fig. 1(c)) and the seven-parameter friction (Fig. 1(d)) (Armstrong-Hélouvry, 1994) will be used in order to interpret the friction at low velocity, e.g. the capsule system (Liu et al. (2013)), the crane system (Fang et al., 2012), and the mass-spring-damping system (Martinez and Alvarez, 2008). The seven-parameter friction model has some nonlinear characteristics, e.g. frictional memory, which are not required in this paper. The friction model adopted in this paper combines the Coulomb and the Stribeck friction models which could sufficiently describe the motion transition between the sticking and slip regimes.

Fig. 2(a) depicts the discontinuous friction model adopted in this paper. Comparing to the models in Fig. 1, it has an extra region $(-\zeta, \zeta)$ which represents the sticking phase and the stick-to-slip transition phase. In some practical engineering systems, e.g. downhole drilling, ground moling, the motion of these systems at very low speed can be approximately considered as stationary. From the numerical simulation point of view, taking such an approximation is necessary as the velocity from the slip to sticking phase may not equal to zero exactly. An example, the stick-slip oscillations of a drill-string system (Liu, 2014), is presented in Fig. 2(b). As can be seen from the figure, drill bit is stuck, $\dot{q}_n = 0$, at the beginning due to $|f_r| < \mu_s \Lambda$. When reaction force is greater than frictional torque, $|f_r| > \mu_s \Lambda$, drill bit starts to rotate and the friction on drill bit is $f = \mu_s \Lambda \operatorname{sgn}(f_r)$ at this occasion. After a short while, bit speed increases drastically, and then reduces rapidly afterwards. Once bit speed falls in the region, $|\dot{q}_n| < \zeta$, drill bit is considered as stationary, so it is stuck again. Since the stick-slip motion may induce harmful oscillations to the entire system, this paper will focus on suppressing such motion by using sliding-mode control.

It is worth noting that the inertia matrix D in Eq. (1) is diagonal, and both the damping matrix

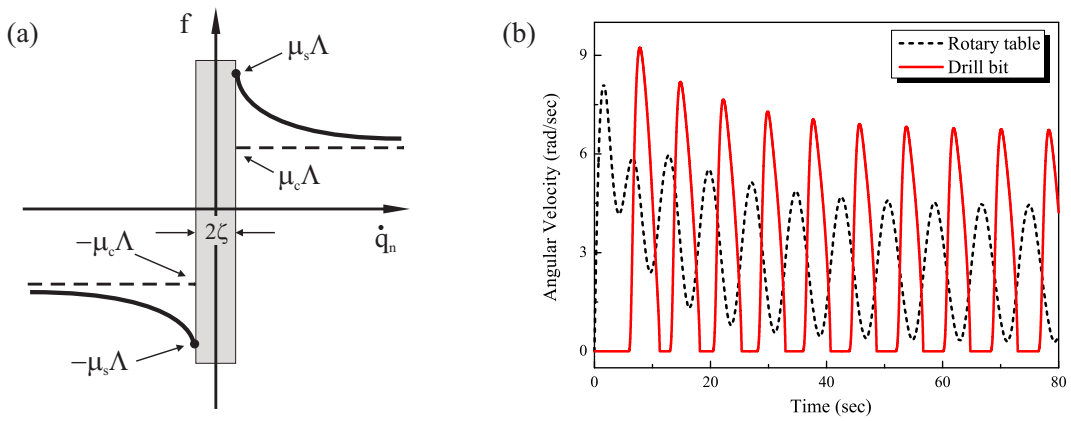

Figure 2: (a) Discontinuous friction in Eq. (2). (b) Stick-slip behaviour of a drill-string system (Liu, 2014).

C and the stiffness matrix K are symmetric. This configuration represents a class of flat multibody underactuated systems (Liu and Yu, 2013), and their configuration variables are coupled by damping and stiffness forces in a chain form. In particular, control input is only applied to the first configuration variable, and the friction model (2) acts on the last one. Relevant applications could be the flexible servo system and the drill-string system for downhole oil and gas exploration. Control of a long drill-string which could run for a few kilometers deep is only controllable through applying control torque to the rotary table on the surface, while drill bit encounters notable frictions in borehole. Hence, maintaining a desired rotary speed and avoiding the stick-slip oscillations for such a long structure become crucial for safety and economical purposes. Readers could refer to (Liu, 2014; Lopez-Martinez et al., 2010; Canudas-de-Wit et al., 2008) for more details.

3. Motion regimes and equilibria

Let Γ be a switching manifold

$$\Gamma := \{q \in \Re^{n\times 1} : \dot{q}_n = 0\} \tag{3}$$

and $\tilde{\Gamma}$ be an attractive region

$$\tilde{\Gamma} := \{q \in \Gamma : |\, c_{n-1}\dot{q}_{n-1} + k_{n-1}(q_{n-1} - q_n)| < \mu_s \Lambda\} \tag{4}$$

which is a subset of Γ. Due to the presence of discontinuous friction (2), three motion regimes of the system, when control input is constant, can be identified as

- Sticking regime: for $\forall t > t_s$, $q \in \tilde{\Gamma}$, where t_s is the time when system trajectory reaches $\tilde{\Gamma}$ and stays in the region thereafter;
- Stick-slip regime: system trajectory enters and leaves $\tilde{\Gamma}$ repeatedly;
- Slip regime: system has an asymptotically stable equilibrium $\bar{x}_p$.

In order to obtain the equilibrium in slip regime $\bar{x}_p$, let us define a new state

$$\begin{aligned} x &= [\dot{q}_1,\ q_1 - q_2,\ \dot{q}_2,\ q_2 - q_3,\ \cdots,\ \dot{q}_{n-1}, q_{n-1} - q_n,\ \dot{q}_n]^T \\ &= [x_1,\ x_2,\ x_3,\ x_4,\ \cdots,\ x_{2n-3},\ x_{2n-2},\ x_{2n-1}]^T, \end{aligned}$$

and the underactuated system (1) can be rewritten as

$$\begin{aligned}
\dot{x}_1 &= \tfrac{1}{d_1}[\,u - c_1(x_1 - x_3) - k_1 x_2], \\
\dot{x}_2 &= x_1 - x_3, \\
\dot{x}_3 &= \tfrac{1}{d_2}[c_1(x_1 - x_3) - c_2(x_3 - x_5) + k_1 x_2 - k_2 x_4], \\
\dot{x}_4 &= x_3 - x_5, \\
&\vdots \qquad\quad \vdots \\
\dot{x}_{2n-3} &= \tfrac{1}{d_{n-1}}[\,c_{n-2}(x_{2n-5} - x_{2n-3}) - c_{n-1}(x_{2n-3} - x_{2n-1}) + k_{n-2}x_{2n-4} - k_{n-1}x_{2n-2}], \\
\dot{x}_{2n-2} &= x_{2n-3} - x_{2n-1}, \\
\dot{x}_{2n-1} &= \tfrac{1}{d_n}[\,c_{n-1}(x_{2n-3} - x_{2n-1}) + k_{n-1}x_{2n-2} - f],
\end{aligned} \tag{5}$$

The following propositions are given.

Proposition 1. *When the system moves in a constant speed x_c, where $|\,x_c| \geq \zeta$, it has an asymptotically stable equilibrium*

$$\bar{x}_p \quad = [x_c, \tfrac{u_c}{k_1}, x_c, \tfrac{u_c}{k_2}, \cdots, x_c, \tfrac{u_c}{k_{n-1}}, x_c]^T,$$

where $u_c = f(x_c)$ is constant.

Proof. Since the system moves in a constant speed $|\,x_c| \geq \zeta$, it gives

$$[\dot{x}_1,\, \dot{x}_2,\, ...,\, \dot{x}_{2n-1}]^T = [0,\, 0,\, ...,\, 0]^T,$$

and we obtain $u_c = f(x_c)$ from Eq. (5). Now, let us define a Lyapunov function

$$\begin{aligned}
\bar{V} \quad &= \tfrac{1}{2}[d_1(x_1 - x_c)^2 + k_1(x_2 - \tfrac{u_c}{k_1})^2 + d_2(x_3 - x_c)^2 + k_2(x_4 - \tfrac{u_c}{k_2})^2 \cdots \\
&\quad + d_{n-1}(x_{2n-3} - x_c)^2 + k_{n-1}(x_{2n-2} - \tfrac{u_c}{k_{n-1}})^2 + d_n(x_{2n-1} - x_c)^2],
\end{aligned} \tag{6}$$

and its time derivative can be written as

$$\begin{aligned}
\dot{\bar{V}} \quad &= d_1(x_1 - x_c)\dot{x}_1 + k_1(x_2 - \tfrac{u_c}{k_1})\dot{x}_2 + d_2(x_3 - x_c)\dot{x}_3 + k_2(x_4 - \tfrac{u_c}{k_2})\dot{x}_4 \cdots \\
&\quad + d_{n-1}(x_{2n-3} - x_c)\dot{x}_{2n-3} + k_{n-1}(x_{2n-2} - \tfrac{u_c}{k_{n-1}})\dot{x}_{2n-2} + d_n(x_{2n-1} - x_c)\dot{x}_{2n-1}.
\end{aligned} \tag{7}$$

Substituting $\dot{x}$ in Eq. (7) using Eq. (5) gives

$$\begin{aligned}
\dot{\bar{V}} \quad &= (x_1 - x_c)[u_c - c_1(x_1 - x_3) - k_1 x_2] + k_1(x_2 - \tfrac{u_c}{k_1})(x_1 - x_3) \\
&\quad + (x_3 - x_c)[c_1(x_1 - x_3) - c_2(x_3 - x_5) + k_1 x_2 - k_2 x_4] \\
&\quad + k_2(x_4 - \tfrac{u_c}{k_2})(x_3 - x_5) \cdots + k_{n-1}(x_{2n-2} - \tfrac{u_c}{k_{n-1}})(x_{2n-3} - x_{2n-1}) \\
&\quad + (x_{2n-1} - x_c)[\,c_{n-1}(x_{2n-3} - x_{2n-1}) + k_{n-1}x_{2n-2} - u_c]
\end{aligned} \tag{8}$$

Simplifying Eq. (8) by removing brackets in the equation gives

$$\begin{aligned}
\dot{\bar{V}} \quad &= -c_1 x_1^2 + 2c_1 x_1 x_3 - c_1 x_3^2 - c_2 x_3^2 + 2c_2 x_3 x_5 - c_2 x_5^2 \cdots \\
&\quad - c_{n-1}x_{2n-3}^2 + 2c_{n-1}x_{2n-3}x_{2n-1} - c_{n-1}x_{2n-1}^2 \\
&= -c_1(x_1 - x_3)^2 - c_2(x_3 - x_5)^2 \cdots - c_{n-1}(x_{2n-3} - x_{2n-1})^2,
\end{aligned} \tag{9}$$

Therefore $\dot{\bar{V}} \leq 0$. Let $\mathcal{G}$ be the set of all points in slip regime where $\dot{\bar{V}} = 0$, and $\mathcal{D}$ be the largest invariant set in $\mathcal{G}$. Since $\dot{\bar{V}} = 0$ only for $x = \bar{x}_p$, the set $\mathcal{D}$ can be expressed as

$$\mathcal{D} := \{x \in \Re^{(2n-1)\times 1} : |\; x = \bar{x}_p\}. \tag{10}$$

By using the LaSalle's Invariance Principle (LaSalle, 1968), every solution starting from slip regime approaches $\mathcal{D}$ as $t \to \infty$. Therefore, the equilibrium $\bar{x}_p$ is asymptotically stable. ■

Remark 1. *It is worth noting that if $x_c = 0$, the system is in sticking regime which has an asymptotically stable equilibrium*

$$\bar{x}_s = [0, \tfrac{u_c}{k_1}, 0, \tfrac{u_c}{k_2}, \cdots, 0, \tfrac{u_c}{k_{n-1}}, 0]^T$$

due to $u_c \leq \mu_s \Lambda$. If $x_c \neq 0$, $u_c = [\mu_c + (\mu_s - \mu_c)e^{-\gamma|x_c|/v_f}]\Lambda \operatorname{sgn}(x_c)$, so the existence of x_c depends on u_c and Λ.

Proposition 2. *Consider the attractive region $\tilde{\Gamma}$ in (4), for a constant control input u_c, if $x_c \neq 0$, the equilibrium $\bar{x}$ exists when $\bar{x} \notin \tilde{\Gamma}$ and selection of the desired equilibrium $\bar{x}_d$ for control purpose should be far away from the boundary of $\tilde{\Gamma}$.*

Proof. For the switching manifold (3), system trajectory will have a sliding mode when $x_{2n-1}\dot{x}_{2n-1} < 0$ leading to $x_{2n-1} \to 0$ as $t \to \infty$. In the case $x_{2n-1} < 0$, $f = \mu_d \Lambda \operatorname{sgn}(x_{2n-1}) < 0$. Since reaction force is less than friction force in sliding mode, i.e. $|f_r| < |f|$, we have

$$|\, c_{n-1}(x_{2n-3} - x_{2n-1}) + k_{n-1}x_{2n-2}| < -f,$$

which is a subset of

$$\mathcal{M}^- := \{x \in \Re^{(2n-1)\times 1} : |\, c_{n-1}x_{2n-3} + k_{n-1}x_{2n-2}| < c_{n-1}|x_{2n-1}| - f\}. \tag{11}$$

In the case $x_{2n-1} > 0$, $f = \mu_d \Lambda$, and the set for sliding mode is a subset of

$$\mathcal{M}^+ := \{x \in \Re^{(2n-1)\times 1} : |\, c_{n-1}x_{2n-3} + k_{n-1}x_{2n-2}| < c_{n-1}|x_{2n-1}| + f\}. \tag{12}$$

Combining (11) and (12), the sliding mode $x_{2n-1}\dot{x}_{2n-1} < 0$ can be guaranteed in the set

$$\mathcal{M} := \{x \in \Re^{(2n-1)\times 1} : |\, c_{n-1}x_{2n-3} + k_{n-1}x_{2n-2}| < c_{n-1}|x_{2n-1}| + [\mu_c + (\mu_s - \mu_c)e^{-\frac{\gamma}{v_f}|x_{2n-1}|}]\Lambda\} \tag{13}$$

Since $\Gamma \subset \mathcal{M}$, system trajectory will be within attractive region $\tilde{\Gamma}$ once it hits switching manifold Γ. Thereafter, either of the following two cases may happen: system trajectory (1) asymptotically converges to $\bar{x}$ at where $x_c = 0$; or (2) enters and leaves $\tilde{\Gamma}$ repeatedly in stick-slip regime. Hence, selection of the desired equilibrium $\bar{x}_d$ should be far away from the boundary of $\tilde{\Gamma}$ for ensuring that control input is sufficiently large to avoid switching manifold Γ. ■

Remark 2. *It should be noted that the underactuated systems studied by Ashrafiuon and Erwin (2008) have one motion regime and global stabilization is available, while the systems considered in this paper have three motion regimes and only local stabilization within slip regime is possible. The control design proposed in this paper is for tracking the desired equilibrium $\bar{x}_d$ in slip regime, while sticking and stick-slip regimes should be avoided.*

4. Sliding-mode controller design

The control goal is to avoid sticking and stick-slip regimes, and force the system to track the desired constant velocity x_d in slip regime. This could be achieved by introducing a sliding surface along which system trajectory enters sliding regime, and then our control goal could be satisfied. Let us define a sliding surface as

$$s = (x_1 - x_d) + \lambda \int_0^t (x_1 - x_d)\, \mathrm{d}\tau + \lambda \int_0^t (x_1 - x_{2n-1})\, \mathrm{d}\tau, \tag{14}$$

where λ is a positive constant selected by designer, and the time derivative of the sliding surface can be written as

$$\dot{s} = \dot{x}_1 + \lambda\,(x_1 - x_d) + \lambda\,(x_1 - x_{2n-1}). \tag{15}$$

It is worth noting that, when system trajectory is on the sliding surface $s = 0$, control target $x_1 \to x_d$ can be guaranteed by the first term in Eq. (14), and the second and third terms may ensure $x_{2n-1} \to x_d$. Thereafter, the rest of variables asymptotically converge to the desired equilibrium which will be proved by Proposition 3 given below.

Next, substituting $\dot{x}_1$ in Eq. (15) using Eq. (5) gives

$$\dot{s} = \tfrac{1}{d_1}[\, u - c_1(x_1 - x_3) - k_1 x_2] + \lambda\,(x_1 - x_d) + \lambda\,(x_1 - x_{2n-1}). \tag{16}$$

The ideal controller without any parametric uncertainty can be derived by equating $\dot{s} = 0$ as

$$\tilde{u} = c_1(x_1 - x_3) + k_1 x_2 - d_1\lambda\,(x_1 - x_d) - d_1\lambda\,(x_1 - x_{2n-1}). \tag{17}$$

Define a sliding-mode controller as

$$u = u_e + u_s, \tag{18}$$

where u_e is an equivalent control, and u_s is a switching control of the sliding-mode controller. Equivalent control could be obtained from Eq. (17) as

$$u_e = \hat{c}_1(x_1 - x_3) + \hat{k}_1 x_2 - \hat{d}_1\lambda\,(x_1 - x_d) - \hat{d}_1\lambda\,(x_1 - x_{2n-1}), \tag{19}$$

where "$\hat{}$" indicates estimated system parameter, and switching control is given by

$$u_s^{\mathrm{I}} = -\sigma \mathrm{sgn}(s), \tag{20}$$

where σ is the reaching control gain associated with the upper bounds of uncertainties, and the discontinuous sign function can be written as

$$\mathrm{sgn}(s) = \begin{cases} 1 & \text{if } s > 0, \\ 0 & \text{if } s = 0, \\ -1 & \text{if } s < 0. \end{cases}$$

Now the following theorem is given.

Theorem 1. *If the upper bounds of the estimated system parameters are known as*

$$|\,\hat{c}_1 - c_1| \le \Delta_c,\ |\,\hat{k}_1 - k_1| \le \Delta_k, |\,\hat{d}_1 - d_1| \le \Delta_d,$$

and the switching control gain is chosen as

$$\sigma = \Delta_c|\,x_1 - x_3| + \Delta_k|\,x_2| + \Delta_d\lambda\,|\,x_1 - x_d| + \Delta_d\lambda\,|\,x_1 - x_{2n-1}| + \eta, \tag{21}$$

where η is a positive constant, by applying the sliding-mode control (18)-(20), any trajectory of the system could reach and stay thereafter on the manifold $s = 0$ in finite time.

Proof. Let choose a Lyapunov function

$$V_1 = \tfrac{1}{2}\, d_1 s^2, \tag{22}$$

and the time derivative of V_1 can be written as

$$\dot{V}_1 = d_1 s\dot{s}. \tag{23}$$

Substituting $\dot{s}$ in Eq. (23) using Eq. (16) gives

$$\dot{V}_1 = s[\, u - c_1(x_1 - x_3) - k_1 x_2 + d_1\lambda\,(x_1 - x_d) + d_1\lambda\,(x_1 - x_{2n-1})]. \tag{24}$$

Applying the sliding-mode controller (18), Eq. (24) becomes

$$\begin{aligned}\dot{V}_1 &= s[(\hat{c}_1 - c_1)(x_1 - x_3) + (\hat{k}_1 - k_1)x_2 \\ &\quad +(d_1 - \hat{d}_1)\lambda(x_1 - x_d) + (d_1 - \hat{d}_1)\lambda(x_1 - x_{2n-1}) - \sigma\mathrm{sgn}(s)].\end{aligned} \tag{25}$$

Since the switching control gain is chosen as Eq. (21), the time derivative of V_1 can be rewritten as

$$\begin{aligned}\dot{V}_1 &= s[(\hat{c}_1 - c_1)(x_1 - x_3) + (\hat{k}_1 - k_1)x_2 \\ &\quad +(d_1 - \hat{d}_1)\lambda(x_1 - x_d) + (d_1 - \hat{d}_1)\lambda(x_1 - x_{2n-1}) \\ &\quad -\Delta_c|x_1 - x_3|\,\mathrm{sgn}(s) - \Delta_k|x_2|\,\mathrm{sgn}(s) \\ &\quad -\Delta_d\lambda|x_1 - x_d|\,\mathrm{sgn}(s) - \Delta_d\lambda|x_1 - x_{2n-1}|\,\mathrm{sgn}(s) - \eta\,\mathrm{sgn}(s)] \\ &\leq -\eta|s| \leq 0.\end{aligned} \tag{26}$$

Therefore, by applying the sliding-mode controller (18)-(20) with the reaching control gain (21), system trajectory could reach and stay thereafter on the manifold $s = 0$ in finite time. ■

Proposition 3. *Once system trajectory stays on the manifold $s = 0$, system state will asymptotically converge to the desired equilibrium*

$$\bar{x}_d = [x_d, \tfrac{\bar{h}_d}{k_1}, x_d, \tfrac{\bar{h}_d}{k_2}, \cdots, x_d, \tfrac{\bar{h}_d}{k_{n-1}}, x_d]^T,$$

where $\bar{h}_d = [\mu_c + (\mu_s - \mu_c)e^{-\gamma|x_d|/v_f}]\Lambda\,\mathrm{sgn}(x_d)$.

Proof. Applying the desired equilibrium $\bar{x}_d$ to the Lyapunov function $\bar{V}$ in Eq. (6) gives

$$\begin{aligned}\bar{V}_d &= \tfrac{1}{2}[d_1(x_1 - x_d)^2 + k_1(x_2 - \tfrac{\bar{h}_d}{k_1})^2 + d_2(x_3 - x_d)^2 + k_2(x_4 - \tfrac{\bar{h}_d}{k_2})^2 \cdots \\ &\quad + d_{n-1}(x_{2n-3} - x_d)^2 + k_{n-1}(x_{2n-2} - \tfrac{\bar{h}_d}{k_{n-1}})^2 + d_n(x_{2n-1} - x_d)^2],\end{aligned} \tag{27}$$

and its time derivative is written as

$$\begin{aligned}\dot{\bar{V}}_d &= d_1(x_1 - x_d)\dot{x}_1 + k_1(x_2 - \tfrac{\bar{h}_d}{k_1})\dot{x}_2 + d_2(x_3 - x_d)\dot{x}_3 + k_2(x_4 - \tfrac{\bar{h}_d}{k_2})\dot{x}_4 \cdots \\ &\quad + d_{n-1}(x_{2n-3} - x_d)\dot{x}_{2n-3} + k_{n-1}(x_{2n-2} - \tfrac{\bar{h}_d}{k_{n-1}})\dot{x}_{2n-2} + d_n(x_{2n-1} - x_d)\dot{x}_{2n-1}.\end{aligned} \tag{28}$$

Since system trajectory is on the sliding surface $s = 0$, the equivalent control equals to the ideal control in Eq. (17). Applying Eq. (5) and (17) to Eq. (28), it gives

$$\dot{\bar{V}}_d = -c_1(x_1 - x_3)^2 - c_2(x_3 - x_5)^2 \cdots - c_{n-1}(x_{2n-3} - x_{2n-1})^2 \leq 0, \tag{29}$$

where $\dot{\bar{V}}_d = 0$ only for $x = \bar{x}_d$. So, the desired equilibrium $\bar{x}_d$ is asymptotically stable once system trajectory stays on the sliding surface $s = 0$. ■

Remark 3. *When system trajectory approaches to the manifold $s = 0$, it is switched around the manifold due to the discontinuous sign function which could lead to high-frequency chattering on control input and thereby on system state.*

In order to overcome this issue, the following theorem is proposed.

Theorem 2. *If the modified switching control*

$$u_s^{\mathrm{II}} = -\sigma\frac{s}{|s| + \delta} - \kappa s \tag{30}$$

is applied, where δ and κ are small positive constants selected by designer, the tracking errors of the system are asymptotically bounded.

Proof. Applying the modified switching control (30), the time derivative of the Lyapunov function (23) becomes

$$\begin{aligned}
\dot{V}_2 &= s[(\hat{c}_1 - c_1)(x_1 - x_3) + (\hat{k}_1 - k_1)x_2 + (d_1 - \hat{d}_1)\lambda\,(x_1 - x_d) \\
&\quad +(d_1 - \hat{d}_1)\lambda\,(x_1 - x_{2n-1}) - \Delta_c|\,x_1 - x_3|\tfrac{s}{|s|+\delta} - \Delta_k|\,x_2|\tfrac{s}{|s|+\delta} \\
&\quad -\Delta_d\lambda\,|x_1 - x_d|\tfrac{s}{|s|+\delta} - \Delta_d\lambda\,|\,x_1 - x_{2n-1}|\tfrac{s}{|s|+\delta} - \eta\tfrac{s}{|s|+\delta} - \kappa s] \\
&\le |s(\hat{c}_1 - c_1)(x_1 - x_3)| + |s(\hat{k}_1 - k_1)x_2| + |s(d_1 - \hat{d}_1)\lambda\,(x_1 - x_d)| \\
&\quad +|s(d_1 - \hat{d}_1)\lambda\,(x_1 - x_{2n-1})| - \Delta_c|\,x_1 - x_3|\tfrac{s^2}{|s|+\delta} - \Delta_k|\,x_2|\tfrac{s^2}{|s|+\delta} \\
&\quad -\Delta_d\lambda\,|x_1 - x_d|\tfrac{s^2}{|s|+\delta} - \Delta_d\lambda\,|\,x_1 - x_{2n-1}|\tfrac{s^2}{|s|+\delta} - \eta\tfrac{s^2}{|s|+\delta} - \kappa s^2 \\
&\le |(\hat{c}_1 - c_1)(x_1 - x_3)|\tfrac{|s|(|s|+\delta)}{|s|+\delta} + |(\hat{k}_1 - k_1)x_2|\tfrac{|s|(|s|+\delta)}{|s|+\delta} \\
&\quad +|(d_1 - \hat{d}_1)\lambda\,(x_1 - x_d)|\tfrac{|s|(|s|+\delta)}{|s|+\delta} + |(d_1 - \hat{d}_1)\lambda\,(x_1 - x_{2n-1})|\tfrac{|s|(|s|+\delta)}{|s|+\delta} \\
&\quad -\Delta_c|\,x_1 - x_3|\tfrac{s^2}{|s|+\delta} - \Delta_k|\,x_2|\tfrac{s^2}{|s|+\delta} - \Delta_d\lambda\,|x_1 - x_d|\tfrac{s^2}{|s|+\delta} \\
&\quad -\Delta_d\lambda\,|\,x_1 - x_{2n-1}|\tfrac{s^2}{|s|+\delta} - \eta\tfrac{s^2}{|s|+\delta} - \kappa s^2 \\
&\le \delta[\,|(\hat{c}_1 - c_1)(x_1 - x_3)| + |(\hat{k}_1 - k_1)x_2| + |(d_1 - \hat{d}_1)\lambda\,(x_1 - x_d)| \\
&\quad +|(d_1 - \hat{d}_1)\lambda\,(x_1 - x_{2n-1})|\,]\tfrac{|s|}{|s|+\delta} - \kappa s^2 \\
&\le \delta[\,|(\hat{c}_1 - c_1)(x_1 - x_3)| + |(\hat{k}_1 - k_1)x_2| + |(d_1 - \hat{d}_1)\lambda\,(x_1 - x_d)| \\
&\quad +|(d_1 - \hat{d}_1)\lambda\,(x_1 - x_{2n-1})|\,] - \kappa s^2.
\end{aligned}$$

This implies that for the set $\mathcal{V} = \{s : \|s\| \le \sqrt{\|\delta\Theta\|/\kappa}\,\}$, it follows that $\dot{V}_2 < 0$, $\forall s \in \mathcal{V}^{\mathsf{c}}$, where $\mathcal{V}^{\mathsf{c}}$ is the complement of $\mathcal{V}$, and Θ is given by

$$\begin{aligned}
\Theta &= |(\hat{c}_1 - c_1)(x_1 - x_3)| + |(\hat{k}_1 - k_1)x_2| + |(d_1 - \hat{d}_1)\lambda\,(x_1 - x_d)| \\
&\quad +|(d_1 - \hat{d}_1)\lambda\,(x_1 - x_{2n-1})|.
\end{aligned}$$

This means that the sliding surface does not tend to zero any more, but is bounded as $\|s\| \le \sqrt{\|\delta\Theta\|/\kappa}$, so the tracking errors of the system become asymptotically bounded. However, there should be a compromise between a little deterioration of the tracking errors and a large reduction of chattering. ■

Remark 4. *The parameter δ can be selected as small as possible such that $\delta \to 0$ leading to $\|s\| \to 0$ so $x \to \bar{x}_d$. However, if the parameter δ is too small, the continuous function $\frac{s}{|s|+\delta}$ becomes discontinuous so that chattering will be introduced to system again.*

Since the modified switching control (30) is only asymptotically bounded, not asymptotically convergent, the following switching control is proposed.

Theorem 3. *If the switching control is chosen as*

$$\begin{aligned}
u_s^{\mathrm{III}} &= -\frac{\Delta_c|x_1 - x_3|s}{|s| + \delta_1 \exp(-\delta_2 \int |x_1 - x_3|\,\mathrm{d}t)} - \frac{\Delta_k|x_2|s}{|s| + \delta_1 \exp(-\delta_2 \int |x_2|\,\mathrm{d}t)} \\
&\quad -\frac{\Delta_d\lambda|x_1 - x_d|s}{|s| + \delta_1 \exp(-\delta_2 \int \lambda|x_1 - x_d|\,\mathrm{d}t)} - \frac{\Delta_d\lambda|x_1 - x_{2n-1}|s}{|s| + \delta_1 \exp(-\delta_2 \int \lambda|x_1 - x_{2n-1}|\,\mathrm{d}t)} - \kappa s,
\end{aligned} \tag{31}$$

where δ_1 and δ_2 are small positive constants selected by designer, system trajectory will reach sliding surface asymptotically, and system state will asymptotically converge to the desired equilibrium $\bar{x}_d$.

Proof. In order to prove the stability of the switching control u_s^{III} (31), a new Lyapunov function is defined as

$$\begin{aligned}
V_3 &= \tfrac{1}{2}\,d_1 s^2 + \Delta_c\tfrac{\delta_1}{\delta_2}\exp(-\delta_2 \int |\,x_1 - x_3|\,\mathrm{d}t) + \Delta_k\tfrac{\delta_1}{\delta_2}\exp(-\delta_2 \int |\,x_2|\,\mathrm{d}t) \\
&\quad +\Delta_d\tfrac{\delta_1}{\delta_2}\exp(-\delta_2 \int \lambda|\,x_1 - x_d|\,\mathrm{d}t) + \Delta_d\tfrac{\delta_1}{\delta_2}\exp(-\delta_2 \int \lambda|\,x_1 - x_{2n-1}|\,\mathrm{d}t).
\end{aligned} \tag{32}$$

From the strict definition of the Lyapunov function, the new function (32) is positive definite, but not a legitimate Lyapunov function, since $\forall t \ge 0$, $V_3(0) \ne 0$. So the following additional state is introduced.

$$z = [\,z_1,\, z_2,\, z_3,\, z_4\,]^T,$$

where

$$\begin{aligned} z_1 &= \sqrt{2\Delta_c \tfrac{\delta_1}{\delta_2} \exp(-\delta_2 \textstyle\int |\, x_1 - x_3|\, \mathrm{d}t)} \\ z_2 &= \sqrt{2\Delta_k \tfrac{\delta_1}{\delta_2} \exp(-\delta_2 \textstyle\int |\, x_2|\, \mathrm{d}t)} \\ z_3 &= \sqrt{2\Delta_d \tfrac{\delta_1}{\delta_2} \exp(-\delta_2 \textstyle\int \lambda |\, x_1 - x_d|\, \mathrm{d}t)} \\ z_4 &= \sqrt{2\Delta_d \tfrac{\delta_1}{\delta_2} \exp(-\delta_2 \textstyle\int \lambda |\, x_1 - x_{2n-1}|\, \mathrm{d}t)}. \end{aligned}$$

Then Eq. (32) becomes

$$V_3 = \tfrac{1}{2}\, d_1 s^2 + \tfrac{1}{2}\, z^T z = \tfrac{1}{2}\, d_1 s^2 + \tfrac{1}{2} \sum_{i=1}^{4} z_i^2. \tag{33}$$

As $t \to \infty$, z_i is exponentially convergent to zero leading to $V_3 \to 0$ when $s = 0$. Hence, Eq. (33) is a legitimate Lyapunov function with state variables $[\, s,\, z^T]^T$, and the time derivative of V_3 is given as

$$\begin{aligned} \dot{V}_3 &= d_1 s \dot{s} - \Delta_c\, \delta_1 |\, x_1 - x_3| \exp(-\delta_2 \textstyle\int |\, x_1 - x_3|\, \mathrm{d}t)) - \Delta_k\, \delta_1 |\, x_2| \exp(-\delta_2 \textstyle\int |\, x_2|\, \mathrm{d}t) \\ &\quad -\Delta_d\, \delta_1 \lambda |\, x_1 - x_d| \exp(-\delta_2 \textstyle\int \lambda |\, x_1 - x_d|\, \mathrm{d}t) \\ &\quad -\Delta_d\, \delta_1 \lambda |\, x_1 - x_{2n-1}| \exp(-\delta_2 \textstyle\int \lambda |\, x_1 - x_{2n-1}|\, \mathrm{d}t). \end{aligned} \tag{34}$$

Applying the sliding-mode control (18) using the equivalent control (19) and the new switching control (31), Eq. (34) becomes

$$\begin{aligned} \dot{V}_3 &= s[(\hat{c}_1 - c_1)(x_1 - x_3) + (\hat{k}_1 - k_1)\, x_2 + (d_1 - \hat{d}_1)\lambda\, (x_1 - x_d) \\ &\quad +(d_1 - \hat{d}_1)\lambda\, (x_1 - x_{2n-1}) - \tfrac{\Delta_c |x_1 - x_3| s}{|s| + \delta_1 \exp(-\delta_2 \int |x_1 - x_3|\, \mathrm{d}t)} - \tfrac{\Delta_k |x_2| s}{|s| + \delta_1 \exp(-\delta_2 \int |x_2|\, \mathrm{d}t)} \\ &\quad -\tfrac{\Delta_d \lambda |x_1 - x_d| s}{|s| + \delta_1 \exp(-\delta_2 \int \lambda |x_1 - x_d|\, \mathrm{d}t)} - \tfrac{\Delta_d \lambda |x_1 - x_{2n-1}| s}{|s| + \delta_1 \exp(-\delta_2 \int \lambda |x_1 - x_{2n-1}|\, \mathrm{d}t)} - \kappa s] \\ &\quad -\Delta_c\, \delta_1 |\, x_1 - x_3| \exp(-\delta_2 \textstyle\int |\, x_1 - x_3|\, \mathrm{d}t)) - \Delta_k\, \delta_1 |\, x_2| \exp(-\delta_2 \textstyle\int |\, x_2|\, \mathrm{d}t) \\ &\quad -\Delta_d\, \delta_1 \lambda |\, x_1 - x_d| \exp(-\delta_2 \textstyle\int \lambda |\, x_1 - x_d|\, \mathrm{d}t) \\ &\quad -\Delta_d\, \delta_1 \lambda |\, x_1 - x_{2n-1}| \exp(-\delta_2 \textstyle\int \lambda |\, x_1 - x_{2n-1}|\, \mathrm{d}t) \\ &\le |(\hat{c}_1 - c_1)(x_1 - x_3) s| + |(\hat{k}_1 - k_1)\, x_2 s| + |(d_1 - \hat{d}_1)\lambda\, (x_1 - x_d) s| \\ &\quad +|(d_1 - \hat{d}_1)\lambda\, (x_1 - x_{2n-1}) s| - \tfrac{\Delta_c |x_1 - x_3| s^2}{|s| + \delta_1 \exp(-\delta_2 \int |x_1 - x_3|\, \mathrm{d}t)} - \tfrac{\Delta_k |x_2| s^2}{|s| + \delta_1 \exp(-\delta_2 \int |x_2|\, \mathrm{d}t)} \\ &\quad -\tfrac{\Delta_d \lambda |x_1 - x_d| s^2}{|s| + \delta_1 \exp(-\delta_2 \int \lambda |x_1 - x_d|\, \mathrm{d}t)} - \tfrac{\Delta_d \lambda |x_1 - x_{2n-1}| s^2}{|s| + \delta_1 \exp(-\delta_2 \int \lambda |x_1 - x_{2n-1}|\, \mathrm{d}t)} - \kappa s^2 \\ &\quad -\Delta_c\, \delta_1 |\, x_1 - x_3| \exp(-\delta_2 \textstyle\int |\, x_1 - x_3|\, \mathrm{d}t)) - \Delta_k\, \delta_1 |\, x_2| \exp(-\delta_2 \textstyle\int |\, x_2|\, \mathrm{d}t) \\ &\quad -\Delta_d\, \delta_1 \lambda |\, x_1 - x_d| \exp(-\delta_2 \textstyle\int \lambda |\, x_1 - x_d|\, \mathrm{d}t) \\ &\quad -\Delta_d\, \delta_1 \lambda |\, x_1 - x_{2n-1}| \exp(-\delta_2 \textstyle\int \lambda |\, x_1 - x_{2n-1}|\, \mathrm{d}t) \\ &\le |(\hat{c}_1 - c_1)\, \delta_1 (x_1 - x_3)| \exp(-\delta_2 \textstyle\int |\, x_1 - x_3|\, \mathrm{d}t) + |(\hat{k}_1 - k_1)\, \delta_1 x_2| \exp(-\delta_2 \textstyle\int |\, x_2|\, \mathrm{d}t) \\ &\quad +|(d_1 - \hat{d}_1)\lambda\, \delta_1 (x_1 - x_d)| \exp(-\delta_2 \textstyle\int \lambda |\, x_1 - x_d|\, \mathrm{d}t) \\ &\quad +|(d_1 - \hat{d}_1)\lambda\, \delta_1 (x_1 - x_{2n-1})| \exp(-\delta_2 \textstyle\int \lambda |\, x_1 - x_{2n-1}|\, \mathrm{d}t) \\ &\quad -\Delta_c\, \delta_1 |\, x_1 - x_3| \exp(-\delta_2 \textstyle\int |\, x_1 - x_3|\, \mathrm{d}t)) - M_k\, \delta_1 |\, x_2| \exp(-\delta_2 \textstyle\int |\, x_2|\, \mathrm{d}t) \\ &\quad -\Delta_d\, \delta_1 \lambda |\, x_1 - x_d| \exp(-\delta_2 \textstyle\int \lambda |\, x_1 - x_d|\, \mathrm{d}t) \\ &\quad -\Delta_d\, \delta_1 \lambda |\, x_1 - x_{2n-1}| \exp(-\delta_2 \textstyle\int \lambda |\, x_1 - x_{2n-1}|\, \mathrm{d}t) - \kappa s^2 \\ &\le -\kappa s^2 \le 0. \end{aligned}$$

Therefore, using the new switching control (31), any system trajectory could reach and stay thereafter on the manifold $s = 0$ asymptotically. According to Proposition 3, system state will eventually converges to the desired equilibrium $\bar{x}_d$ asymptotically. ■

Remark 5. *The parameter δ_1 can be selected according to the selection of δ in Remark 4, and the parameter δ_2 determines the decay rate of the exponential function* $\exp(\cdot)$ *in Eq. (31), so it should be chosen relatively smaller for avoiding chattering effect.*

5. Simulation studies

In order to validate the proposed controllers, two underactuated mechanical systems, a mass-spring-damping system and a drill-string system are used for simulation studies. Both of the systems could be extended from 2-DOF to multi-DOF with discontinuous friction acting on the n^{th} body, and the control objective for them is to track a desired velocity for all the configuration variables in the presence of parametric uncertainties.

5.1. The mass-spring-damping system

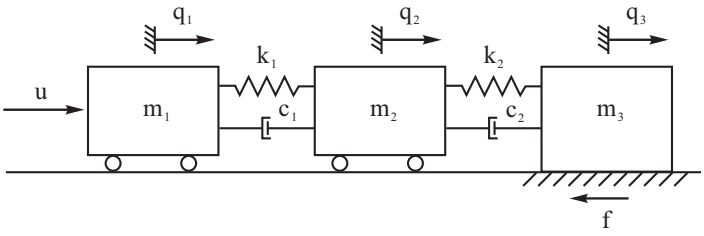

Figure 3: A mass-spring-damping system

Consider the system shown in Figure 3, which consists of three masses, m_1, m_2, and m_3 connected by the springs k_1, k_2 and the dampers c_1, c_2. A control force u is applied to the first mass, m_1 and the third mass, m_3 is subjected to a discontinuous friction f given by

$$f = \begin{cases} f_r & \text{if } |\dot{q}_3| < \zeta \text{ and } |f_r| \leq f_s, \\ \mu_s m_3 g \operatorname{sgn}(f_r) & \text{if } |\dot{q}_3| < \zeta \text{ and } |f_r| > f_s, \\ \mu_d m_3 g \operatorname{sgn}(\dot{q}_3) & \text{if } |\dot{q}_3| \geq \zeta, \end{cases}$$

where $g = 9.8$ m/s^2 is the acceleration due to gravity. The displacements of the masses m_1, m_2, and m_3 are q_1, q_2, and q_3, respectively. The equations of motion for the mass-spring-damping system are written as

$$\begin{cases} m_1\ddot{q}_1 + c_1\dot{q}_1 - c_1\dot{q}_2 + k_1 q_1 - k_1 q_2 = u, \\ m_2\ddot{q}_2 - c_1\dot{q}_1 + (c_1 + c_2)\,\dot{q}_2 - c_2\dot{q}_3 - k_1 q_1 + (k_1 + k_2)\,q_2 - k_2 q_3 = 0, \\ m_3\ddot{q}_3 - c_2\dot{q}_2 + c_2\dot{q}_3 - k_2 q_2 + k_2 q_3 + f = 0, \end{cases} \tag{35}$$

where the model parameters are given as $m_1 = 1$ kg, $m_2 = 1$ kg, $m_3 = 0.5$ kg, $k_1 = 0.5$ N/m, $k_2 = 0.5$ N/m, $c_1 = 0.1$ Ns/m, and $c_2 = 0.1$ Ns/m, and the physical parameters for the discontinuous friction f are $\zeta = 10^{-6}$ m/s, $\mu_s = 0.3$, $\mu_c = 0.1$, $\gamma = 0.8$, and $v_f = 1$ m/s. The estimated model parameters used for the controllers are $\hat{m}_1 = 1.1$ kg, $\hat{k}_1 = 0.8$ N/m, and $\hat{c}_1 = 0.2$ Ns/m, and their upper bounds were chosen as $\Delta_{m1} = 0.2$ kg, $\Delta_{k1} = 0.4$ N/m, and $\Delta_{c1} = 0.2$ Ns/m. The control parameters, $\delta = 0.01$, $\delta_1 = 0.01$, and $\delta_2 = 10^{-5}$ were used in numerical simulations.

The simulation results for tracking a desired speed $\dot{q}_d = 2$ m/sec are shown in Fig. 4. It can be seen from the figure that the third mass m_3 has stick-slip motion initially and the system is stabilized to the desired speed after the control is switched on at $t = 30$ seconds. However, the discontinuous sign function in Theorem 1 results in chattering effect on the first mass m_1 as shown in Fig. 4(a). A blow-up window clearly shows the chattering on $\dot{q}_1$ when system trajectory approaches to the sliding surface $s = 0$. The control inputs from the proposed controllers are compared in Fig. 5, where the chattering control input by Theorem 1 can be clearly observed. Comparing the rates of convergence of the proposed controllers,

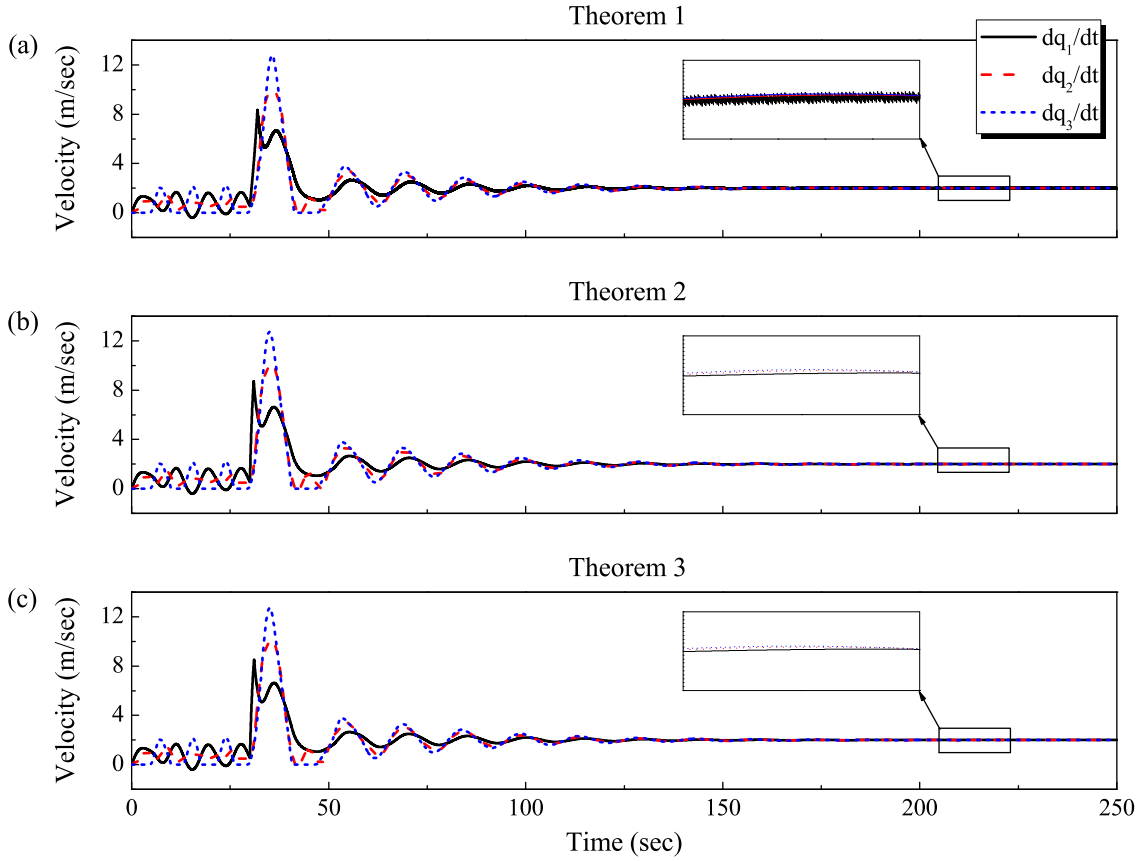

Figure 4: Time histories of mass velocities, $\dot{q}_1$ (solid lines), $\dot{q}_2$ (dash lines), and $\dot{q}_3$ (short dash lines) by using (a) Theorem 1, (b) Theorem 2, and (c) Theorem 3. The control is switched on at $t = 30$ seconds.

time histories of the sliding surfaces are shown in Fig. 6. As can be seen from the figure, Theorem 2 has the fastest rate of convergence, while Theorem 1 is the slowest one.

According to Theorem 2, the modified switching control u_s^{II} is asymptotically bounded and the bounded surface may be affected by the constant δ due to $\|s\| \leq \sqrt{\|\delta\Theta\|}/\kappa$. The simulation results with different δ are presented in Fig. 7, where the desired speed was chosen as $\dot{q}_d = 5$ m/sec and the rest of parameters were kept the same as before. It can be seen from Fig. 7(a) that, as δ increases, the overshoot of $\dot{q}_3$ becomes larger and its settling time gets longer. It can be observed from Fig. 7(b) that when δ is greater, the bounded surface becomes more obvious. The bounded convergence could also be

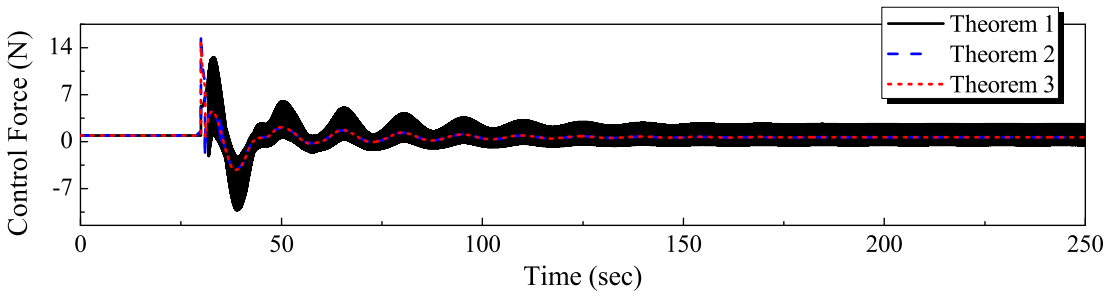

Figure 5: Time histories of control inputs by using Theorem 1 (solid line), Theorem 2 (dash line), and Theorem 3 (short dash line)

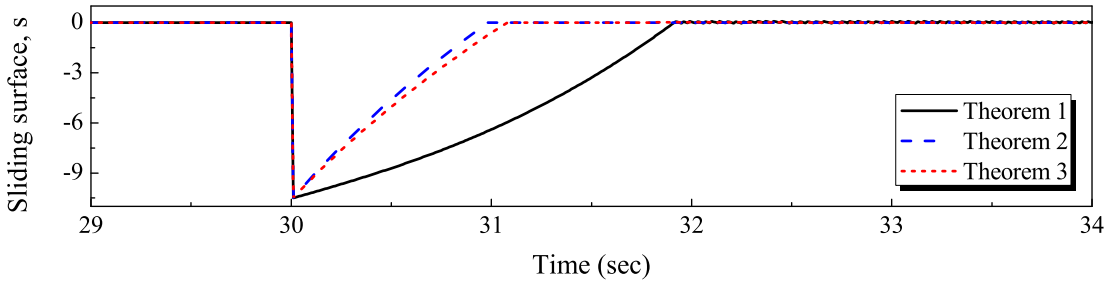

Figure 6: Time histories of sliding surfaces by using Theorem 1 (solid line), Theorem 2 (dash line), and Theorem 3 (short dash line)

observed from Fig. 7(c), where the blow-up window clearly shows that the trajectory for $\delta = 20$ does not approach to the desired equilibrium asymptotically.

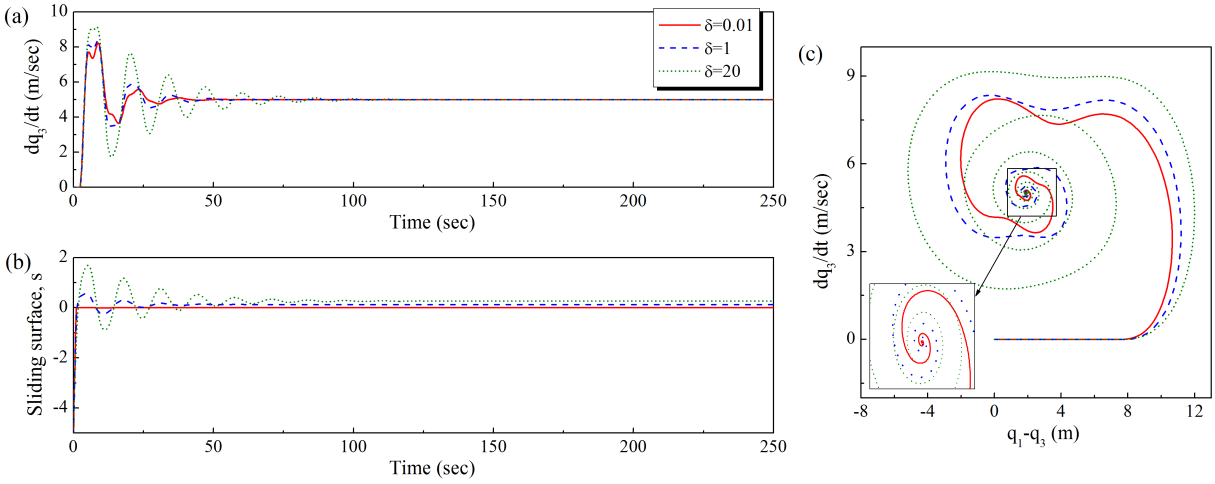

Figure 7: Time histories of (a) mass velocity $\dot{q}_3$, (b) sliding surfaces s, and (c) system trajectories on the phase plane (q_1-q_3, $\dot{q}_3$) by using Theorem 2 with $\delta = 0.01$ (solid line), $\delta = 1$ (dash line), and $\delta = 20$ (dot line).

5.2. The drill-string system

A simplified drill-string system is shown in Fig. 8 which comprises a rotary table, a drill pipe, a drill collar, and a drill bit. The drill-string is a 4-DOF underactuated system, but could be extended to multi-DOF depending on the length of the drill pipe. The equations of motion are written as

$$\begin{cases} J_t\ddot{\phi}_t + c_p\dot{\phi}_t - c_p\dot{\phi}_1 + k_p\phi_t - k_p\phi_1 = u, \\ J_1\ddot{\phi}_1 - c_p\dot{\phi}_t + (c_p + c_r)\dot{\phi}_1 - c_r\dot{\phi}_r - k_p\phi_t + (k_p + k_r)\phi_1 - k_r\phi_r = 0, \\ J_r\ddot{\phi}_r - c_r\dot{\phi}_1 + (c_r + c_b)\dot{\phi}_r - c_b\dot{\phi}_b - k_r\phi_1 + (k_r + k_b)\phi_r - k_b\phi_b = 0, \\ J_b\ddot{\phi}_b - c_b\dot{\phi}_r + c_b\dot{\phi}_b - k_b\phi_r + k_b\phi_b + T_b = 0, \end{cases} \tag{36}$$

where J_i $(i = t,\ 1,\ r,\ b)$ is the disk inertia, c_i $(i = p,\ r,\ b)$ is the torsional damping, k_i $(i = p,\ r,\ b)$ is the torsional stiffness, and T_b is the frictional torque when drill bit contacts with borehole given by

$$T_b = \begin{cases} \tau_r & \text{if } |\dot{\phi}_b| < \zeta \text{ and } |\tau_r| \le \tau_s, \\ \tau_s \mathrm{sgn}(\tau_r) & \text{if } |\dot{\phi}_b| < \zeta \text{ and } |\tau_r| > \tau_s, \\ \mu_d R_b W_{ob}\, \mathrm{sgn}(\dot{\phi}_b) & \text{if } |\dot{\phi}_b| \ge \zeta. \end{cases} \tag{37}$$

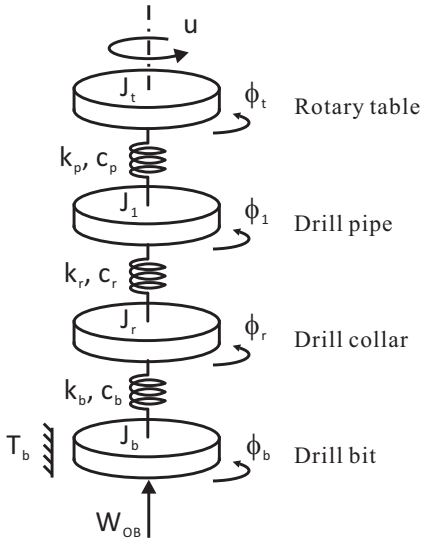

Figure 8: A drill-string system

where the reaction torque $\tau_r = c_b(\dot{\phi}_r - \dot{\phi}_b) + k_b(\phi_r - \phi_b)$, the static friction torque $\tau_s = \mu_s R_b W_{ob}$, R_b is the bit radius, and W_{ob} is the weight-on-bit. The system parameters used in the simulation are given in Table 1. The estimated model parameters used in the proposed controllers are $\hat{J}_t = 800\,\mathrm{kgm}^2$, $\hat{c}_p = 120\,\mathrm{Nms/rad}$, and $\hat{k}_p = 630\,\mathrm{Nm/rad}$, and their upper bounds were chosen as $\Delta_{jt} = 150\,\mathrm{kgm}^2$, $\Delta_{cp} = 40\,\mathrm{Nms/rad}$, and $\Delta_{kp} = 100\,\mathrm{Nm/rad}$. The control parameters, $\delta = 0.01$, $\delta_1 = 0.01$, and $\delta_2 = 10^{-5}$ were used in numerical simulations.

Parameter	Value
J_t	910 kg m^2
J_1	2800 kg m^2
J_r	750 kg m^2
J_b	450 kg m^2
c_p	150 N m s/rad
c_r	190 N m s/rad
c_b	180 N m s/rad
k_p	700 N m/rad
k_r	1080 N m/rad
k_b	910 N m/rad
μ_s	0.8
μ_c	0.45
W_{ob}	30 kN
R_b	0.15 m
γ	0.85
v_f	1 rad/s
ζ	10^{-6} rad/s

Table 1: Model parameters of the drill-string

Time histories of the angular velocities of the rotary table and the drill bit by using the proposed controllers for tracking a desired angular velocity $\dot{\phi}_d = 3$ rad/sec are presented in Fig. 9. As can be seen from the figure, the system undergoes stick-slip motion when no control is applied. Once the controller is switched on at $t = 33$ seconds, the angular velocities of the rotary table and the drill bit asymptotically converge to the desired angular velocity. A further comparison of the proposed controllers

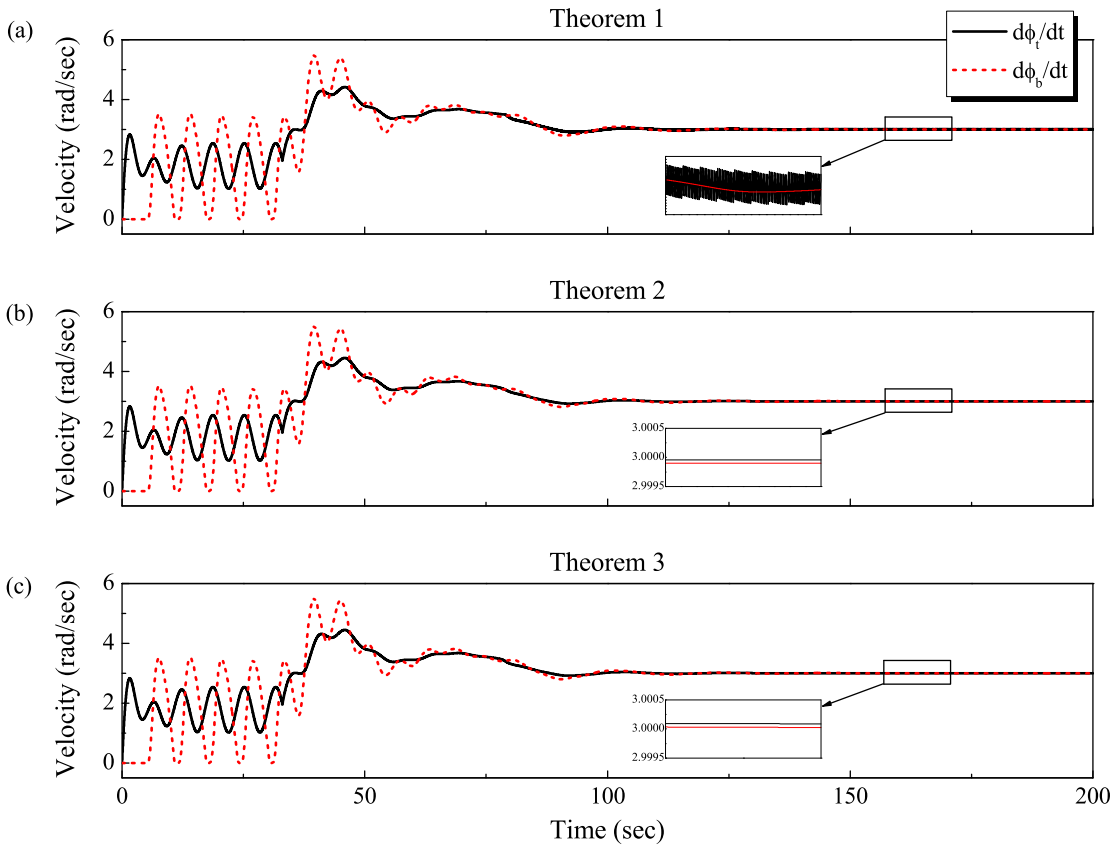

Figure 9: Time histories of the angular velocities of the rotary table, $\dot{\phi}_t$ (solid lines) and the drill bit $\dot{\phi}_b$ (short dash lines) by using (a) Theorem 1, (b) Theorem 2, and (c) Theorem 3 which the control is switched on at $t = 33$ seconds.

is made by using the blow-up windows at where the system has been stabilized. It is seen from the blow-up window in Fig. 9(a) Theorem 1 leads to chattering on the rotary table due to the discontinuous switching function. The blow-up windows in Fig. 9(b) and (c) demonstrate that the tracking errors of Theorem 2 is asymptotically bounded, while Theorem 3 provides a better accuracy of tracking. The control torques generated by the proposed controllers are compared in Fig. 10, where large amplitude of chattering by Theorem 1 could be observed and the chattering inputs have been significantly reduced by the other two controllers. Fig. 11 shows drill-string trajectories on the phase plane $(\phi_t - \phi_b,\ \dot{\phi}_b)$. It can be seen from the figure that the system experiences stick-slip motion at the beginning and these trajectories asymptotically converge to the desired equilibrium when the controllers are switched on.

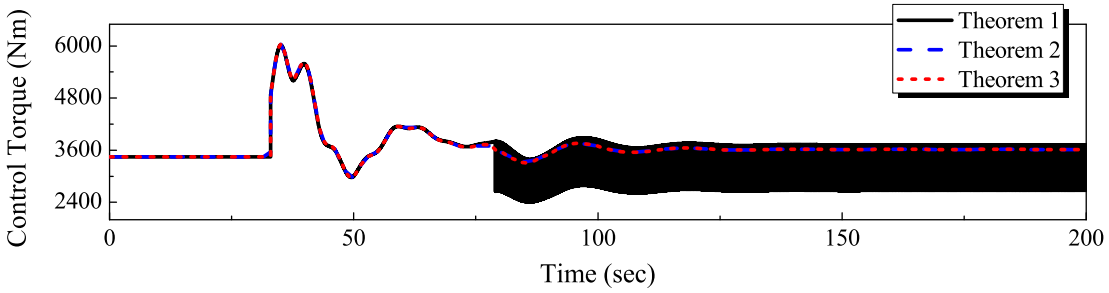

Figure 10: Time histories of control torques by using Theorem 1 (solid line), Theorem 2 (dash line), and Theorem 3 (short dash line)

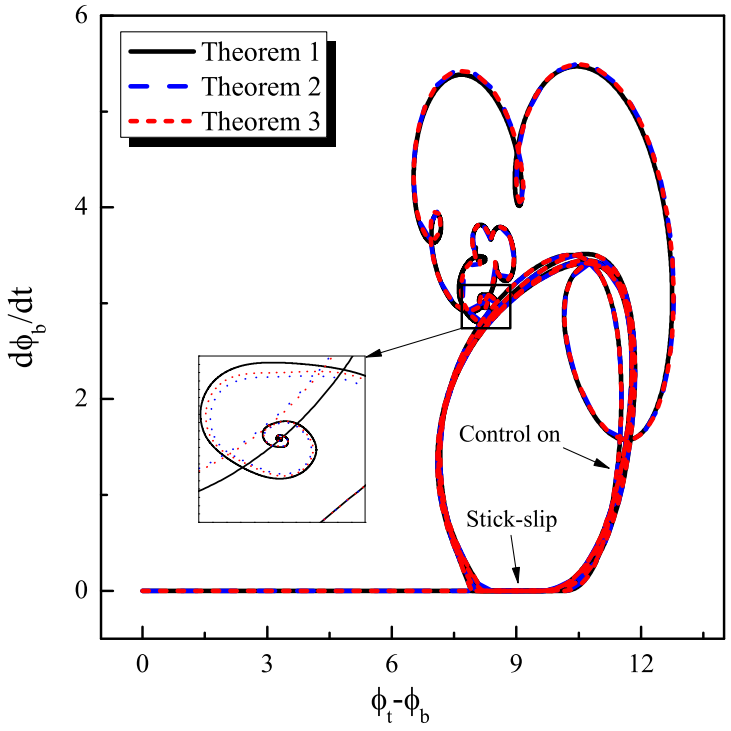

Figure 11: Trajectories of the drill-string on the phase plane ($\phi_t - \phi_b$, $\dot{\phi}_b$) by using Theorem 1 (solid line), Theorem 2 (dash line), and Theorem 3 (short dash line)

6. Conclusions

Stabilization of a class of underactuated systems with discontinuous friction was studied in this paper. This class system has multi-DOF, but only one control input, and the presence of discontinuous friction on unactuated configuration variable leads to the fact that global stabilization is not available. Global motion regimes for this class system, including sticking, stick-slip, and slip were analyzed, and their corresponding equilibria were identified. The control objective was to avoid sticking and stick-slip regimes while tracking a desired equilibrium in slip regime with parametric uncertainties. Three sliding-mode controllers were studied, and their stabilities were proved by using the Lyapunov direct method, which ensures that any system trajectory could reach and stay thereafter on the sliding surface where the desired equilibrium is asymptotically stable. Our first proposed controller was based on the traditional switching control using discontinuous sign function which could induce chattering phenomenon to system. To overcome this issue, a modified switching controller was studied using a continuous function. Although system trajectory may not go to the designed sliding surface anymore, it is asymptotically bounded and control performance still can be achieved. In order to address this problem, the third switching controller was studied to guarantee asymptotical convergence for the system. Simulation results for the mass-spring-damping system and the drill-string system were given to validate the effectiveness of the proposed controllers.

References

Almutairi N. B and Zribi M (2009) Sliding mode control of a three-dimensional overhead crane, *Journal of Vibration and Control* 15: 1679-1730.

Almutairi N. B and Zribi M (2010) On the sliding mode control of a ball on a beam system, *Nonlinear Dynamics* 59: 221-238.

Armstrong-Hélouvry B, Dupont P and de Wit C. C (1994) A survey of models, analysis tools and compensation methods for the control of machines with friction, *Automatica* 30: 1083-1138.

Ashrafiuon H and Erwin R. S (2005) Shape change maneuvers for attitude control of underactuated satellites, in *the American Control Conference*, Portland, OR, USA, pp. 895-900.

Ashrafiuon H and Erwin R. S (2008) Sliding mode control of underactuated multibody systems and its application to shape change control, *International Journal of Control*, 81: 1849-1858.

Ashrafiuon H, Muske K. R, McNinch L. C and Soltan R. A (2008) Sliding-mode tracking control of suerface vessels, *IEEE Transactions on Industrial Eletronics* 55: 4004-4012.

Brockett R. W (1983) Differential Geometric Control Theory, Boston, *MA: Birkhauser*, Ch. Asymptotic stability and feedback stabilization.

Canudas-de-Wit C, Rubio F. R and Corchero M. A (2008) D-OSKIL: a new mechanism for controlling stick-slip oscillations in oil well drillstrings, *IEEE. Trans. Control Systems Technology* 16: 1177-1191.

Egeland O, Dalsmo M and Sordalen O. J (1996) Feedback control of an nonholonomic underwater vehicle with constant desired configuration, *International Journal of Robotics Research* 15: 24-35.

Fahimi F (2007) Sliding-mode formation control for underactuated surface vessels, *IEEE Trans Robotics* 23: 617-622.

Fang Y, Ma B, Wang P, Zhang X (2012) A motion planning-based adaptive control method for an underactuated crane system, *IEEE Trans. Control Systems Technology* 20: 241-248.

Ghommam J, Mnif F and Derbel N (2010) Global stabilisation and tracking control of underactuated surface vessels, *IET Control Theory Appl* 4: 71-88.

Gosselin C, Pelletier F and Laliberte T (2008) An anthropomorphic underactuated robotic hand with 15 DOFs and a single actuator, in *the IEEE International Conference on Robotics and Automation*, Pasadena, CA, USA, pp. 749-754.

Hamed K and Grizzle J (2014) Event-based stabilization of periodic orbits for underactuated 3-D bipedal robots with left-right symmetry, *IEEE Trans. Robotics* 30: 365-381.

Hao Y. X, Yi J. Q, Zhao D. B and Qian D. W (2008) Robust control using incremental sliding mode for underactuated systems with mismatched uncertainties, in *the American Control Conference*, Seattle, Washington, USA, pp. 532-537.

Ho J, Nguyen V and Woo K (2011) Nonlinear dynamics of a new eletro-vibro-impact system, *Nonlinear Dyn.* 63: 35-49.

Hu Y, Yan G and Lin Z (2010) Stable running of a planar underactuated biped robot, *Robotica* 29: 657-665.

Huang J, Guan Z. H, Matsuno T, Fukuda T and Sekiyama K (2010) Sliding-mode velocity control of mobile-wheeled inverted-pendulum systems, *IEEE Transactions on Robotics* 26: 750-758.

LaSalle J. P (1968) Stability theory for ordinary differential equations, *J. Differential Equations* 4: 57-65.

Li E, Liang Z, Hou Z and Tan M (2009) Energy-based balance control approach to the ball and beam system, *International Journal of Control*, 82: 981-992.

Liljebäck P, Pettersen K, Stavdahl Ø and Gravdahl J (2011) Controllability and stability analysis of planar snake robot locomotion, *IEEE Trans. Automatic Control*, 56: 1365-1380.

Liu X, Yu X, Ma G and Xi H (2016) On sliding mode control for networked control systems with semi-Markovian switching and random sensor delays, *Information Sciences*, 337-338: 44-58.

Liu Y, Pavlovskaia E, Hendry D and Wiercigroch M (2013) Vibro-impact responses of capsule system with various friction models, *Int J Mechanical Sciences* 72: 39-54.

Liu Y and Yu H (2013) A survey of underactuated mechanical systems, *IET Control Theory Appl*, 7: 921-935.

Liu Y (2014) Suppressing stick-slip oscillations in underactuated multibody drill-strings with parametric uncertainties using sliding-mode control, *IET Control Theory Appl*, 9: 91-102.

Liu Y and Pavlovskaia E, Wiercigroch M and Peng Z. K (2015) Forward and backward motion control of a vibro-impact capsule system, *Int. J. Non-Linear Mechanics*, 70: 30-46.

Lopez-Martinez M, Acosta J. A and Cano J. M (2010) Non-linear sliding mode surfaces for a class of underactuated mechanical systems, *IET Control Theory and Applications* 4: 2195-2204.

Martinez R and Alvarez J (2008) A controller for 2-DOF underactuated mechanical systems with discontinuous friction, *Nonlinear Dynamics* 53: 191-200.

Martinez R, Alvarez J and Orlov J (2008) Hybrid sliding-mode-based control of underactuated systems with dry frictions, *IEEE Transaction on Industrial Electronics* 55: 3998-4003.

Márton L, Hodel A. S, Lantos B and Hung J. Y (2008) Underactuated robot control: comparing LQR, subspace stabilization, and combined error metric approaches, *IEEE Trans. Industrial Electronics* 55: 3724-3730.

Muskinja N and Tovornik B (2006) Swinging up and stabilization of a real inverted pendulum, *IEEE Trans. Industrial Electronics* 53: 631-639.

Nikkhah M, Ashrafiuon H and Fahimi F (2007) Robust control of underactuated bipeds using sliding modes, *Robotica* 25: 367-374.

Olfati-Saber R (2001) Nonlinear control of underactuated mechanical systems with application to robotics and aerospace vehicles, *Ph.D. thesis*, Department of Electrical Engineering and Computer, Massachusetts Institute of Technology.

Olsson H and Åström K (2001) Friction generated limit cycles, *IEEE Transaction on Control Systems Technology*, 9: 629-636.

Oriolo G and Nakamura Y (1991) Control of mechanical systems with second-order nonholonomic contstraints: Underactuated manipulators, in *the IEEE International Conference on Decision and Control*, Brighton, UK, pp. 2398-2403.

Reyhanoglu M, Schaft A, McClamroch N. H and Kolmanovsky I (1999) Dynamics and control of a class of underactuated mechanical systems, *IEEE Transaction on Automatic Control*, 44: 1663-1671.

Sankaranarayanan V and Mahindrakar A. D (2009) Control of a class of underactuated mechanical systems using sliding modes, *IEEE Transaction on Robotics* 25: 459-467.

She J, Zhang A, Lai X and Wu M (2012) Global stabilization of 2-DOF underactuated mechanical systems - an equivalent-input-disturbance approach, *Nonlinear Dynamics* 69: 495-509.

Spong M. W (1996) Energy based control of a class of underactuated mechanical systems, in *the IFAC World Congress*, San Francisco, CA, USA, pp.431-435.

Vartholomeos P and Papadopoulos E (2005) Dynamics, design and simulation of a novel microrobotic platform employing vibration microactuators, *J. Dyn. Sys., Meas., Control.* 128: 122-133.

Wang W, Yi J, Zhao D and Liu D (2004) Design of a stable sliding-mode controller for a class of second-order underactuated systems, *IEE Procceding on Control Theory Applications* 151: 683-690.

Xu J. X, Guo Z. Q and Lee T. H (2014) Design and implementation of integral slidingmode control on an underactuated two-wheeled mobile robot, *IEEE Trans Industrial Electronics* 61: 3671-3681.

Xu R and Özgüner U (2008) Sliding mode control of a class of underactuated systems, *Automatica* 44: 233-241.

Yue M, Hu P and Sun W (2010) Path following of a class of non-holonomic mobile robot with underactuated vehicle body, *IET Control Theory and Applications* 4: 1898-1904.